

Carriers in a two-dimensional lattice under magnetic and electric fields

H. N. Nazareno

International Center of Condensed Matter Physics, Universidade de Brasília-P.O. Box 04513, 70910-900 Brasília-DF, Brazil

P. E. de Brito

Universidade Católica de Brasília, Departamento de Física, Campus Águas Claras, 72030-070 Brasília-DF, Brazil

(Received 12 February 2001; published 3 July 2001)

We have studied the propagation of carriers in a two-dimensional system under the influence of magnetic and electric fields. To take into account the magnetic field we have used the Peierls substitution, and have considered the so-called Landau gauge for the vector potential. The nature of the propagation of the wave packet under only a magnetic field is controlled by the ratio between the magnetic flux through the unit cell to the flux quantum: $\alpha = \Phi/\Phi_0$. For rational values of α we have obtained ballistic propagation for sufficient long times. But for irrational α the wave remains localized in a definite region due to incommensurability. The inclusion of the electric field changes this picture. In fact, when the electric field is included, the degeneracy between the on-site energies is broken along the field direction, thus inhibiting hopping along it, while in the *perpendicular* direction to the applied field propagation is favored. This behavior is common to both rational and irrational α . Finally, for certain values of the electric and magnetic fields the wave packet performs an oscillatory movement; this is the phenomenon of *dynamic localization*.

DOI: 10.1103/PhysRevB.64.045112

PACS number(s): 71.70.Di, 72.15.Rn, 73.21.-b

I. INTRODUCTION

The object of the present work is to analyze the combined effect of magnetic and electric fields on propagation of carriers subject to a two-dimensional periodic potential. The subject of electrons in a periodic potential under magnetic fields has a long and rich history.¹⁻⁴ Recently there was a renewed interest in dealing with carriers in a two-dimensional system under electric and magnetic fields, due to the fact that it has become recently experimentally accessible.⁵⁻⁸

In dealing with a magnetic field we determine the time evolution of a wave packet in a two-dimensional crystalline array following the Peierls approximation. We shall limit our study to the case of a single band, i.e., large gaps and/or magnetic-field intensities such that no interband mixing occurs. It is well known by now through a classical work by Hofstadter that the eigenvalues of this model follows a self-similar pattern. There are bands and gaps at all energy scales. A crucial parameter that determines the nature of the spectrum is the ratio α of the magnetic flux through a unit cell to the flux quantum unit $\Phi_0 = hc/e$. We face a problem of commensurability, since the magnetic field requires a quantification of areas, while the lattice periodic potential requires the translational symmetry of the crystal. These conditions become compatible only at specific values of the magnetic field. We show different types of propagation according to the nature of the parameter α . In fact, for rational values we obtain *ballistic* propagation for sufficient long times, while for the case in which α is irrational the wave packet remains *localized* in a definite region of the lattice as a consequence of incommensurability. To determine the type of propagation of an injected particle in the lattice, we evaluate the mean-square displacement, the participation function, and the Shannon entropy. In addition, we look at the time evolution of the wave packet in three-dimensional (3D) graphs. In this

work we take the Hamiltonian to be the one given by the Peierls model.

Two situations arise as a consequence of the superposition of the fields. First, the wave presents a tendency to propagate *perpendicular* to the applied electric field. Second, for specific values of the parameters involved, we obtain a resonance condition which makes the packet perform an oscillatory movement with a characteristic period, this is the phenomenon of dynamical localization. In order to gain an explanation for this phenomenon, we have analyzed the density of states for different values of α and the electric field. Our results show the appearance of a series of gaps in the spectrum, whenever the wave packet is localized.

The paper is organized as follows. First we present a Peierls model that allows us to treat the problem of a carrier in a periodic potential subject to a magnetic field which was treated along the Landau gauge. Finally, we consider the inclusion of a dc electric field superimposed on the magnetic field. This will cause the introduction of an additional term into the Hamiltonian, which will be responsible for, among other things, the phenomenon of dynamical localization.

II. PEIERLS MODEL

The time-dependent nonrelativistic equation for a two-dimensional particle of charge e in a periodic potential with an applied magnetic field is

$$i\hbar \frac{d\Psi}{dt} = \frac{1}{2m} (-i\hbar \nabla - e\mathbf{A}/c)^2 \Psi + V(x,y) \Psi, \quad (1)$$

where \mathbf{A} is the vector potential and V is periodic with the periodicity of the lattice. The corresponding stationary Schrödinger equation is

$$\frac{1}{2m}(-i\hbar\nabla - e\mathbf{A}/c)^2\varphi + V(x,y)\varphi = E\varphi. \quad (2)$$

If we call φ_0 the eigenfunction of the Hamiltonian without a magnetic field, the associated wave function φ , when the field is included, is

$$\varphi = \varphi_0 \exp\left(\frac{-ie}{\hbar c} \oint \mathbf{A} \cdot d\mathbf{r}\right) = \varphi_0 \exp(-2\pi i\alpha). \quad (3)$$

Taking the circulation along a unit cell, we see the appearance of the ratio of the magnetic flux through the cell to the quantum flux unit, $\alpha = \Phi/\Phi_0$ in the exponent. When this ratio is an integer, we preserve the original translational symmetry of the lattice, the wave function being single valued. But when α is a rational number, i.e., $\alpha = p/q$ we shall need to consider a unit cell q times as large. Consequently, the Brillouin zone is reduced by the same amount, and there appear q bands. The original single band is split into as many bands as the denominator in α .⁹ This is the origin of the famous butterfly spectrum obtained by Hofstadter.¹⁰ The unconventional features of such a spectrum arise when the magnetic flux through the unit cell becomes comparable to the flux quantum.

Now we shall consider the time evolution of a wave packet in a magnetic field following the Peierls model.¹ According to this, as the Hamiltonian one takes the dispersion relation

$$E(\mathbf{k}) = 2W(\cos k_x a + \cos k_y a), \quad (4)$$

and makes the substitution

$$\hbar\mathbf{k} \Rightarrow \mathbf{\Pi} = -i\hbar\nabla - e\mathbf{A}/c. \quad (5)$$

In this work we have adopted the Landau gauge $\mathbf{A} = B(0,x)$. By discretizing the space coordinates,

$$x = na, \quad y = ma,$$

we expand the wave function in the Wannier representation

$$|\Psi(t)\rangle = \sum_{n,m} g_{n,m}(t)|n,m\rangle,$$

so that from Eq. (1) for a square lattice of $N \times N$ sites, we obtain the following set of equations:

$$i\hbar \frac{dg_{n,m}}{dt} = W[g_{n+1,m} + g_{n-1,m} + e^{-ian}g_{n,m+1} + e^{ian}g_{n,m-1}]. \quad (6)$$

In the Appendix we discuss the properties of the 1D system obtained as a consequence of the Landau gauge.

Equation (6) can be cast in the matrix form

$$i\hbar \frac{d\mathbf{F}}{dt} = \mathbf{M}\mathbf{F}, \quad (7)$$

where \mathbf{M} is the dynamical matrix, and the vector $F(i;t)$ is constructed from the Wannier amplitudes $g_{n,m}(t)$ by taking, as the first N components of the vector \mathbf{F} the first row of the $N \times N$ matrix formed with the Wannier amplitudes of the

different sites. The next N components (from $N+1$ up to $2N$) are formed with the second row of the matrix, and so on until we obtain the $N \times N$ component of \mathbf{F} .¹¹ We have considered the initial condition

$$g_{n,m}(t=0) = \delta_{n,0}\delta_{m,0}.$$

In a previous work,¹² we showed that the solution of Eq. (7) can be cast in the form

$$\mathbf{F}(t) = \mathbf{R}^t \exp(-i\mathbf{D}t/\hbar)\mathbf{R}\mathbf{F}(0), \quad (8)$$

where \mathbf{D} is the diagonal form of the dynamical matrix $\mathbf{M} = \mathbf{R}^t\mathbf{D}\mathbf{R}$. After solving for the Wannier amplitudes we construct the following.

(i) The mean-square displacement (MSD) $\langle r^2 \rangle$, which in units of the lattice parameter is

$$\langle r^2 \rangle(t) = \sum_{n,m} |g(n,m;t)|^2(n^2 + m^2). \quad (9)$$

(ii) The participation function

$$P(t) = \left\{ \sum_{n,m} |g(n,m;t)|^4 \right\}^{-1}, \quad (10)$$

that indicates the site's participation in the wave function. Since the wave function is normalized, $P=1$ if the wave function is completely localized at a single site, and $P=N$ if the wave is uniformly extended over the N sites in the lattice.¹³ An interesting feature of this function is that it presents an abrupt decline once the packet reaches the boundary of the lattice. In this way we can note the presence of size effects, and enable us to choose the lattice size in order to avoid boundary effects. In addition, since this function keeps track of the number of sites that the wave "visits" it will show oscillations due to backward and forward scattering the wave suffers when reaching a site.

(iii) The Shannon (information) entropy¹⁴

$$S(t) = - \sum_{n,m} |g(n,m;t)|^2 \ln |g(n,m;t)|^2, \quad (11)$$

that takes the two limiting values: $S=0$ for a completely localized state and $\ln N$ for a uniformly extended state.

(iv) We analyze the time evolution of the wave packet in 3D graphics, showing in this way more clearly the nature of propagation (localization).

This approach to the study of diffusion of an initially localized state follows along the lines presented by Anderson;¹⁵ that is, we can conclude that diffusion has occurred if at $t \rightarrow \infty$ the Wannier amplitude at the starting site goes to zero. If, on the other hand, the amplitude at the site remains finite while decreasing rapidly with distance, we say we have a localized state.

III. RATIONAL VS IRRATIONAL MAGNETIC FIELDS

As stated above, when α is rational we have a periodic on-site potential with a q periodicity. But if α is irrational we have an incommensurate potential. Let us discuss first the rational case.

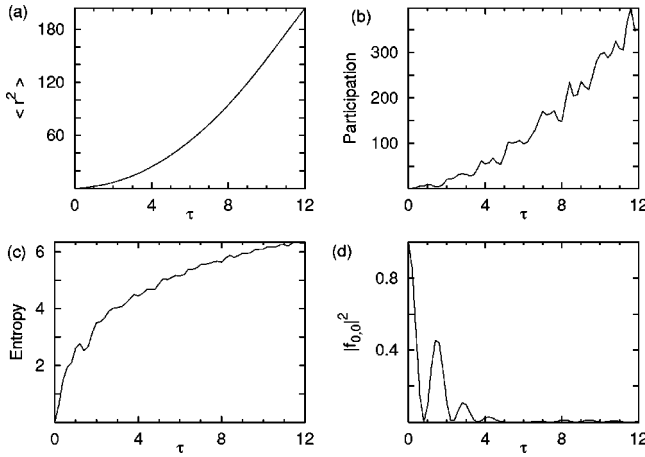


FIG. 1. Rational case: $\alpha=1/2$, without electric field. (a) Mean-square displacement $\langle r^2 \rangle$. (b) Participation. (c) Entropy. (d) Probability propagation at the origin $|f_{0,0}(t)|^2$. Time is in units of \hbar/W .

(i) Rational case: $\alpha=1/2$. In Fig. 1 we show the time evolution of the MSD, participation, entropy, and probability propagation at the origin $|f_{0,0}(t)|^2$. We note that the propagation takes place ballistically, i.e., $\langle r^2 \rangle \propto t^2$. The participation grows linearly in time on the average. The propagator at the origin decays rapidly in time, making the propagation of the wave evident.

In Fig. 2 we show the structure of the wave packet as time goes by. Note that the structure of the picks shows a close resemblance to the circular orbits obtained in the classical description of a charged particle in a magnetic field.¹⁶

(ii) Irrational case: $\alpha=\sigma$ (golden mean $[\sqrt{5}-1]/2$). In Fig. 3 we show the time evolution of the MSD, participation, entropy, and probability propagation at the origin. The MSD shows smaller values than in the rational case. It grows in time because of the “escape” of the wave packet tail. There also appear strong oscillations in the participation and the entropy because of the tendency of the wave packet to return to the origin, as we can see in Fig. 4. In this figure we can very clearly note a breathing mode: the packet expands and contracts.

We have shown results for two typical cases, $\alpha=1/2$ and

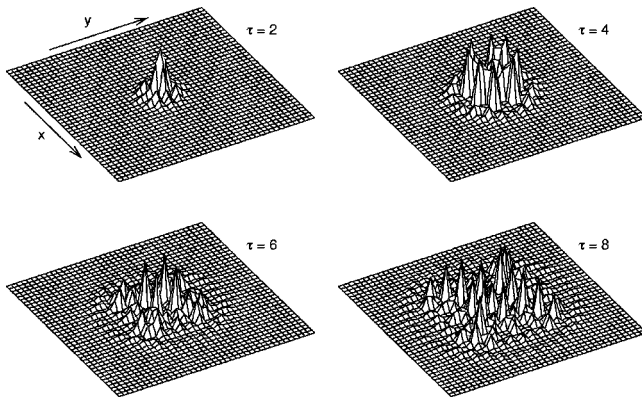


FIG. 2. The structure of the wave packet for $\alpha=1/2$ and $\vec{E}=0$. Time is in units of \hbar/W .

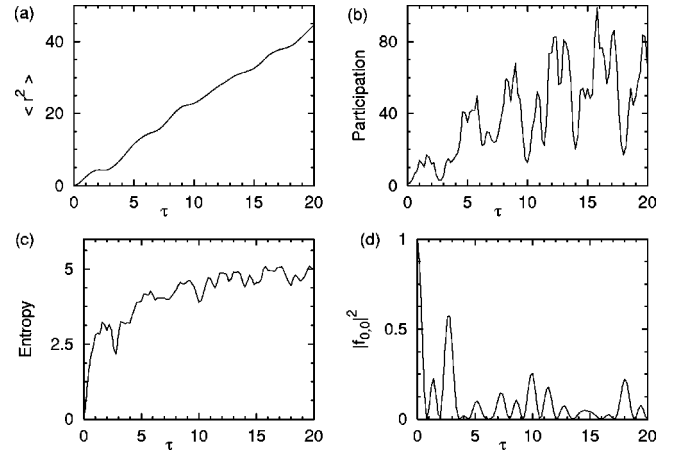


FIG. 3. Irrational case: $\alpha=\sigma$ the (golden mean is $[\sqrt{5}-1]/2$), without electric field. (a) Mean-square displacement $\langle r^2 \rangle$. (b) Participation. (c) Entropy. (d) Probability propagation at the origin $|f_{0,0}(t)|^2$. Time is in units of \hbar/W .

$\alpha=\sigma$, representatives of the rational and irrational cases. Moreover, we have done the calculation for other α values, obtaining similar behaviors. This is a consequence of the commensurability problem cited above.

IV. EFFECT OF THE INCLUSION OF AN ELECTRIC FIELD

Finally, we introduce a dc electric field $\mathbf{E}=(E_x, E_y)$ in the calculations. The units of the electric field are W/ea . In a previous work,¹¹ we showed the effect of its inclusion on the nature of carrier propagation on both 2D and 3D structures. Now we treat the combined effect produced by the magnetic and electric fields. In doing this we add to the right-hand side of the Schrödinger equation (6) the term $(eE_x an + eE_y am)g(n, m)$.

The inclusion of the electric field removes the degeneracy of the on-site levels along its direction. This way the packet has a tendency to propagate in a direction *perpendicular* to the applied field. This behavior can easily be seen in the next 3D figures. We will discuss four typical situations.

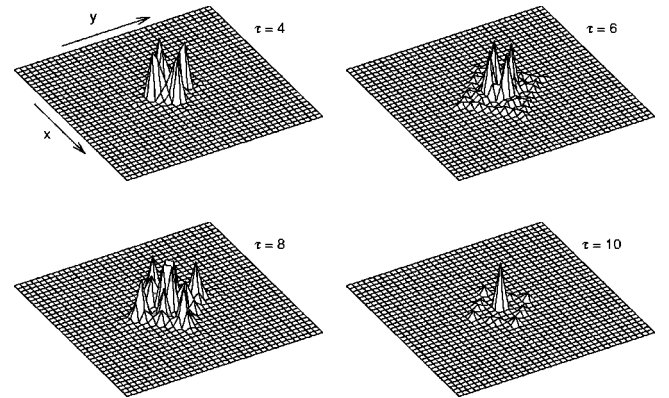


FIG. 4. The structure of the wave packet for $\alpha=\sigma$ and $\vec{E}=0$. Time is in units of \hbar/W .

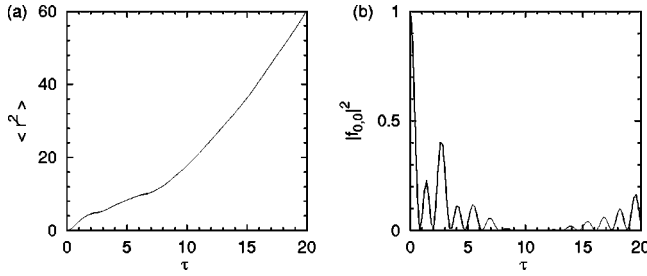


FIG. 5. $\alpha = \sigma$ and $\vec{E} = 0.3\hat{x} + 0.3\hat{y}$ (a) Mean-square displacement $\langle r^2 \rangle$. (b) Probability propagation at the origin $|f_{0,0}(t)|^2$. Time is in units of \hbar/W .

(i) $\vec{E} = 0.3\hat{x} + 0.3\hat{y}$ and $\alpha = \sigma$. In Fig. 5 we show the MSD and probability propagator at the origin, which show that the packet leaves the starting position propagating through the lattice. This behavior is different from the one obtained without the electric field, where the packet remains in a definite region. However, in the present case it is interesting to note that a small portion of the wave packet propagates in direction perpendicular to the applied electric field. See Fig. 6.

(ii) $\vec{E} = 0.5\hat{x}$ and $\alpha = 1/2$. As in the previous situation the wave propagates, as shown in Fig. 7, where one can note that the MSD values are larger than in case (i), where α was irrational. In Fig. 8 we show the wave-packet structure, and it is clearly seen that it goes in the y direction, i.e., perpendicular to the applied field.

Now we will discuss a very interesting situation obtained for rational α , namely, the phenomenon of dynamical localization that occurs for specific values of the electric and magnetic fields. For this we present two situations that illustrate the point.

(iii) $\vec{E} = 0.8\hat{x} + 0.8\hat{y}$ and $\alpha = 1/3$. In Fig. 9 we present the MSD, the probability at the origin, and the density of states (DOS). In Figs. 9(a) and 9(b) we note that the MSD clearly shows a ballistic behavior, while the probability at the origin decays rapidly in time. In Fig. 9(c) the DOS shows a series of peaks without the presence of gaps. This is consistent with the obtained picture of wave propagation. In Fig. 10 we can see the wave leaving the starting position, again in a direction perpendicular to the applied electric field.

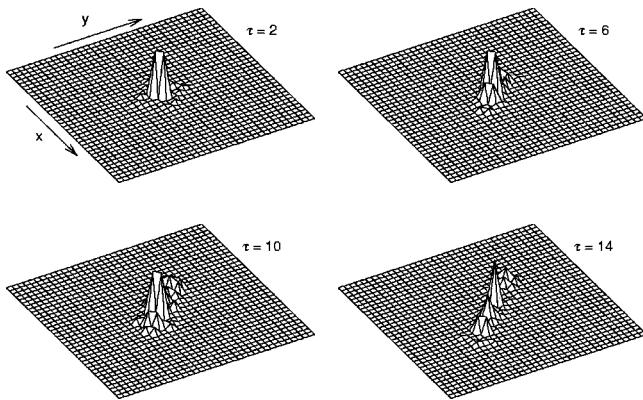


FIG. 6. The structure of the wave packet for $\vec{E} = 0.3\hat{x} + 0.3\hat{y}$ and $\alpha = \sigma$. Time is in units of \hbar/W .

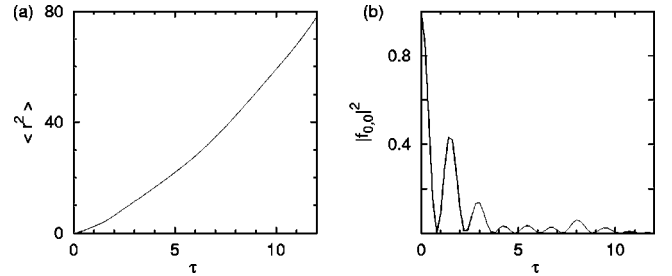


FIG. 7. $\alpha = 1/2$ and $\vec{E} = 0.5\hat{x}$ (a) Mean-square displacement $\langle r^2 \rangle$. (b) Probability propagation at the origin $|f_{0,0}(t)|^2$. Time is in units of \hbar/W .

(iv) $\vec{E} = 0.8\hat{x} + 0.8\hat{y}$ and $\alpha = 1/2$. In this case we realize that a completely different behavior is obtained for this particular set of values of the parameters involved. In Fig. 11(a) we clearly note an oscillatory behavior, while in Fig. 11(b) we see that the particle returns to the origin periodically. In Fig. 11(c) the density of states shows very narrow bands separated by gaps of the same magnitude, while the centers of the minibands are equidistant, the separation being eEa . This is the signature of the Stark ladder structure. It is the presence of these gaps that inhibits hopping from taking place, and as a consequence we end up with a dynamically localized wave packet. Figure 12 shows the packet structure at different times.

The physics behind the very interesting phenomenon of dynamic localization can be stated as follows. Here we discuss the case $\alpha = 1/2$, which means that the translational symmetry is preserved as long as we have another unit cell twice as large while in the presence of only a magnetic field. In this case the wave packet propagates through the lattice, as shown in Fig. 2. The spread of the wave shows a *circular* symmetry resembling a classical orbit. The inclusion of the dc electric field, on the other hand, breaks such a symmetry favoring propagation along the direction *perpendicular* to the applied electric field. Thus we are in the presence of two competing effects. The stronger the field, the more pronounced this asymmetric effect is. Thus if we start with a weak electric field the wave has a tendency to show a circular symmetry, since the Stark ladder that inhibits hopping

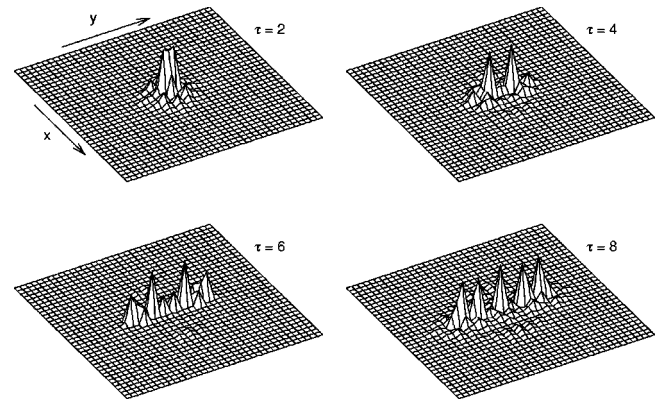


FIG. 8. The structure of the wave packet for $\vec{E} = 0.5\hat{x}$ and $\alpha = 1/2$. Time is in units of \hbar/W .

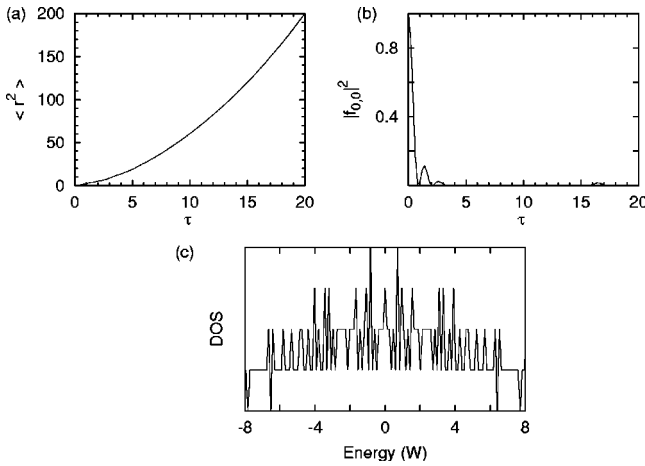


FIG. 9. $\alpha=1/3$ and $\vec{E}=0.8\hat{x}+0.8\hat{y}$. (a) Mean-square displacement $\langle r^2 \rangle$. (b) Probability propagation at the origin ($|f_{0,0}(t)|^2$). (c) DOS—density of states. Time is in units of \hbar/W .

along the field direction produces small barriers. For strong electric fields, on the other hand, the Stark ladder introduces large barriers, severely inhibiting propagation along the applied field. As a result the wave spreads easily along the perpendicular direction, the “escape route” for the carrier is the perpendicular direction pushed by the magnetic field. For some intermediate electric-field intensity, the wave cannot “decide” which behavior to follow, and stays confined to a definite region in the lattice, performing a perfect oscillatory movement. This dynamic localization phenomenon occurs as a result of the balance of two competing effects. Moreover, for the case we illustrate in Figs. 11 and 12, which shows this effect for $\alpha=1/2$ and $E_x=E_y=0.8$, we have obtained a density of states which shows the presence of very narrow minibands separated by gaps of magnitude eEa (see Fig. 11). Thus the presence of these gaps is another manifestation of the fact that the wave packet cannot propagate through the structure. In conclusion, the present calculation seems to indicate that for every rational α a specific electric-field intensity produces dynamical localization as a result of the superposition of both fields acting on Bloch electrons.

We have considered lattices large enough so that the so-

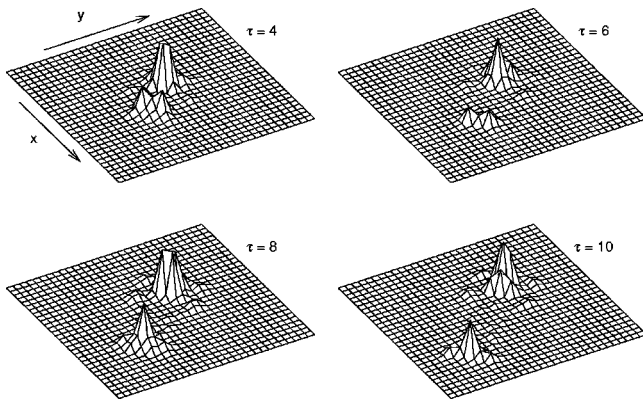


FIG. 10. The structure of the wave packet for $\alpha=1/3$ and $\vec{E}=0.8\hat{x}+0.8\hat{y}$. Time is in units of \hbar/W .

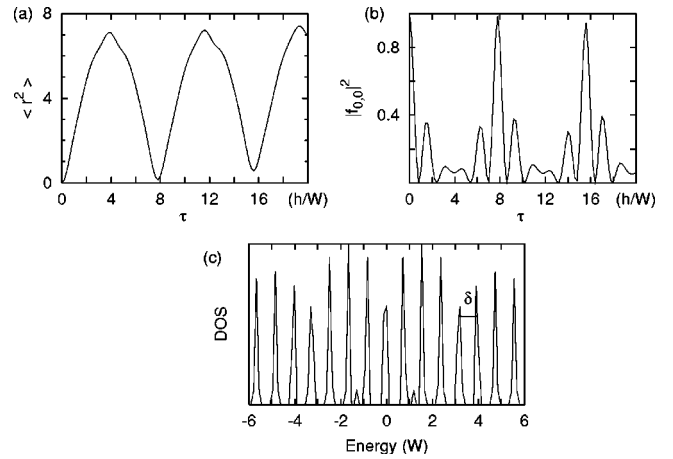


FIG. 11. $\alpha=1/2$ and $\vec{E}=0.8\hat{x}+0.8\hat{y}$ (a) Mean-square displacement $\langle r^2 \rangle$. (b) Probability propagation at the origin ($|f_{0,0}(t)|^2$). (c) DOS—density of states. Time is in units of \hbar/W and $\delta=eEa/W$.

lutions of the Schrödinger equation are size independent. The time limit taken in our calculations was 10^{-9} sec, much longer than any reasonable collision time in a sample.

V. CONCLUSIONS

We have analyzed the influence on propagation of a charged particle injected at a particular site in a two-dimensional lattice under the effect of constant magnetic and electric fields and a crystal potential. We assumed a Peierls model, and considered a Landau gauge for the vector potential. In the absence of an electric field we showed that the parameter which determines the kind of propagation (localization) is the ratio between the magnetic flux through the unit cell to the quantum flux, $\alpha=\Phi/\Phi_0$. When α is a rational number the propagation is *ballistic* for sufficient long times. This can be explained by noting that in this case it is recovered commensurability. Because of this we have a periodic situation though with a different periodicity, and the presence of the hopping term is responsible for this behavior. In the case when α is irrational, we face incommensurability, and the wave packet remains *localized* in a definite region of the lattice. When an electric field is included, this picture is

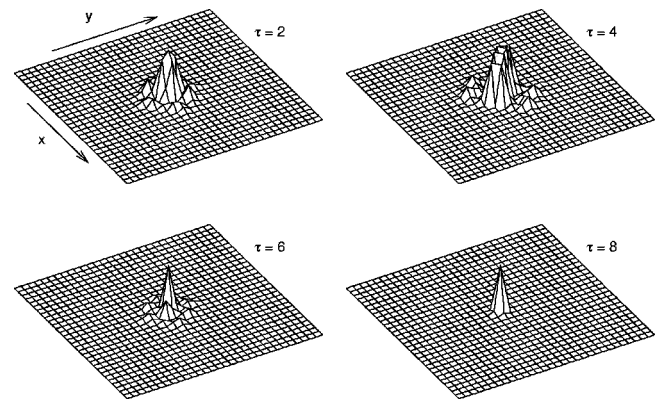


FIG. 12. The structure of the wave packet for $\alpha=1/2$ and $\vec{E}=0.8\hat{x}+0.8\hat{y}$. Time is in units of \hbar/W .

dramatically changed. In fact, since degeneracy between on-site levels along the direction of the applied field is removed, it favors propagation in a *perpendicular* direction. This behavior is common to both rational and irrational α . Our results are in agreement with those obtained by Kunold and Torres,⁵ that showed a change in the energy spectrum with the inclusion of the electric field. Their calculation showed the appearance of a ladder structure, which in turn explained why the wave propagates perpendicularly to the electric field. Note that in the absence of an electric field and for irrational α , the wave remains localized. Moreover, only for specific values of α and E is a localization of the wave packet obtained, where the mean-square displacement $\langle r^2 \rangle$ shows a perfect oscillatory behavior: the wave visits the starting position periodically; this is the phenomenon of *dynamical localization*. For this case the density of states shows the appearance of very narrow minibands separated by gaps of magnitude eEa .

ACKNOWLEDGMENT

H.N.N. would like to thank the Brazilian Agency CNPq for partial support.

APPENDIX: EQUIVALENT 1D PROBLEM

Since in this gauge the vector potential depends only on x , we can assume a plane wave along y . This leads us to the following set of equations for the Wannier amplitudes

$$i\hbar \frac{df_n^\nu}{dt} = W(f_{n+1}^\nu + f_{n-1}^\nu) + 2W \cos(2\pi n\alpha - \nu)f_n^\nu, \quad (\text{A1})$$

where the phase $\nu = k_y a$ is associated with the momentum along the y direction.

The corresponding eigenvalue equation is

$$W(f_{n+1}^\nu + f_{n-1}^\nu) + 2W \cos(2\pi n\alpha - \nu)f_n^\nu = E f_n^\nu, \quad (\text{A2})$$

which gives rise to the Hofstadter spectrum when taking the union of the energy spectra for every ν . This equation is identical to the Aubry model equation,^{17–20} but with a phase on the diagonal term. In addition, since the modulation amplitude is twice the hopping term, the criterion for self-duality is satisfied.²¹ The crucial parameter in the Aubry model is the ratio η between the amplitude of the on-site energies and twice the hopping term. When η is less than 1, a wave packet propagates in the lattice while when η is greater than 1 is in the localization regime. In the present case we are at exactly the critical value $\eta = 1$. Propagation of a particle in the Aubry model was analyzed in a previous work under the presence of a dc electric field.²² In order to incorporate the initial condition $|\Psi(0)\rangle$ we need to solve Eq. (6) for different ν values in the Brillouin zone, and perform the linear combination.

$$g_{n,m}(t) = \frac{1}{N} \sum_{\nu} \exp(i\nu m) f_n^\nu(t).$$

-
- ¹R. E. Peierls, Z. Phys. **80**, 763 (1933).
²L. Onsager, Philos. Mag. **43**, 1006 (1952).
³G. H. Wannier, Rev. Mod. Phys. **34**, 645 (1962).
⁴J. Zak, Phys. Rev. **134**, A1602 (1964).
⁵A. Kunold and M. Torres, Phys. Rev. B **61**, 9879 (2000).
⁶R. Ketzmerick, K. Kruse, D. Springsguth, and T. Geisel, Phys. Rev. Lett. **84**, 2929 (2000).
⁷I. V. Krasovsky, Phys. Rev. Lett. **85**, 4920 (2000).
⁸C. Albrecht, J. H. Smet, D. Weiss, K. von Klitzing, R. Hennig, M. Langenbuch, M. Suhrke, U. Rössler, V. Umansky, and H. Schweizer, Phys. Rev. Lett. **83**, 2234 (1999).
⁹P. M. Chaikin, M. Ya. Azbel, and P. Bak, in *Low-Dimensional Conductors and Superconductors*, edited by D. Jerome and L. G. Caron (Plenum Press, New York, 1987).
¹⁰D. R. Hofstadter, Phys. Rev. B **14**, 2239 (1976).
¹¹H. N. Nazareno and Y. Lepine, Phys. Rev. B **55**, 6661 (1997).
¹²H. N. Nazareno, C. A. A. da Silva, and P. E. de Brito, Phys. Rev. B **50**, 4503 (1994).
¹³F. Wegner, Z. Phys. B: Condens. Matter **36**, 209 (1980).
¹⁴C. E. Shannon, Bell Syst. Tech. J. **27**, 379 (1948).
¹⁵P. W. Anderson, Phys. **109**, 1492 (1958).
¹⁶L. Landau and E. Lifchitz, Quantum Mechanics (Pergamon Press Oxford, 1987); B. H. Bransden and C. J. Joachain, *Quantum Mechanics* (World Scientific, Singapore, 1989); A. P. Balachandran, E. Ercolesi, G. Morandi, and A. M. Srivastava, *Hubbard Model and Anyon Superconductivity* (World Scientific, Singapore, 1990); T. Chakraborty and P. Pietilainen, *The Quantum Hall Effect*, 2nd ed. (Springer, New York, 1995).
¹⁷J. B. Sokoloff, Phys. Rep. **126**, 189 (1985).
¹⁸S. Aubry and G. Andre, Ann. Isr. Phys. Soc. **3**, 133 (1980).
¹⁹E. N. Economou, O. Yanovitskii, and Th. Fraggis, Phys. Rev. B **47**, 740 (1993).
²⁰M. Ya. Azbel, Zh. Eksp. Teor. Fis. **46**, 939 (1964) [Sov. Phys. JETP **19**, 634 (1964)].
²¹Magnus Johansson and Rolf Riklund, Phys. Rev. B **43**, 13 468 (1991).
²²H. N. Nazareno, P. E. de Brito, and C. A. A. da Silva, Phys. Rev. B **51**, 864 (1995).